Self-equilibrium Analysis of Cable Structures based on Isogeometric Analysis

***Keigo Harada[1], Jingyao Zhang[2], Toshiyuki Ogawa[1]**

[1]Department of Architecture and Building Engineering, Tokyo Institute of Technology, 2-12-1 O-okayama, Meguro-ku, 152-8550, Tokyo, Japan
[2]Department of Design and Architecture, Nagoya City University, 2-1-10 Kita-chikusa, Chikusa-ku, Nagoya, 464-0083, Japan

*Keigo Harada: harada.k.ad@m.titech.ac.jp

Abstract

Non-linear analysis of cable structures is computationally expensive due to large deformation against external loads. The Isogeometric Analysis method (IGA) initially developed by T.J.R. Hughes is considered to be more efficient than the existing numerical methods for large-deformation analysis of cable structures. Moreover, Isogeometric Analysis is well suited for the structures with curved configurations, because the same mathematical descriptions for the geometry in the design (CAD) and the modeling in the analysis (FEA) are used. In this paper, we consider the self-equilibrium analysis of catenary cables as well as parabolic cables by using Isogeometric Analysis. The results demonstrate effectiveness and accuracy of Isogeometric Analysis for large deformation analysis of unstable structures, compared to the existing analysis methods.

Keywords: Cable structures, Finite element analysis, Isogeometric analysis, B-spline curve, Self-equilibrium analysis, Singular value decomposition

Introduction

There is a big gap between (computer aided) design (CAD) and analysis in conventional finite element analysis (FEA). This comes from the fact that they are using different mathematical descriptions for the geometry. The gap becomes critical for curved structures, such as shells and cable structures, because their geometries are much complex. To solve the gap by using the same mathematical description for both design and analysis, Hughes et al. (2005; 2009) and thereafter many other researchers developed a new analysis tool, called Isogeometric Analysis method (IGA). Furthermore, smoothness in the curved structures can also be guaranteed in IGA.
The Isogeometric Analysis has been extensively applied for the studies on shell and plate structures, see for example those by Stefan et al. (2011) and Benson et al. (2010). However, there are only a limited number of studies on cables by using IGA. In this paper, we will apply IGA for self-equilibrium analysis of cables under gravity, and investigate its efficiency as well as accuracy by comparison with conventional FEA.

B-spline curve

IGA and conventional FEA share almost the same analysis procedure, except that they use different shape functions. The same mathematical descriptions in (CAD) design, for example B-spline or NURBS curves (surfaces), are used as shape functions in IGA. In the following, we adopt B-spline curves as shape functions, which are constructed by taking a linear combination of B-spline basis functions. The vector-valued coefficients of the basis functions are referred to as control points. A piecewise-polynomial B-spline curve is given by

$$C(\xi) = \sum_{i=1}^{n} N_{i,p}(\xi)\, \mathbf{B}_i \tag{1}$$

where n is the number of control points, p is the polynomial order, ξ_i is the local coordinate of the i^{th} knot, and $\mathbf{B}_i$ is the (global) coordinates of the i^{th} control point. Moreover, the basis functions $N_{i,p}(\xi)$ are defined as follows:

$$N_{i,0}(\xi) = \begin{cases} 1 & \text{if } \xi_i \le \xi < \xi_{i+1} \\ 0 & \text{otherwise} \end{cases}$$
$$N_{i,p}(\xi) = \frac{\xi - \xi_i}{\xi_{i+p} - \xi_i} N_{i,p-1}(\xi) + \frac{\xi_{i+p+1} - \xi}{\xi_{i+p+1} - \xi_{i+1}} N_{i+1,p-1}(\xi) \tag{2}$$

Eq. (2) is referred to as the Cox-de Boor recursion formula (Cox, 1971; de Boor, 1972). Piecewise linear interpolation of the control points gives the so-called control polygon.

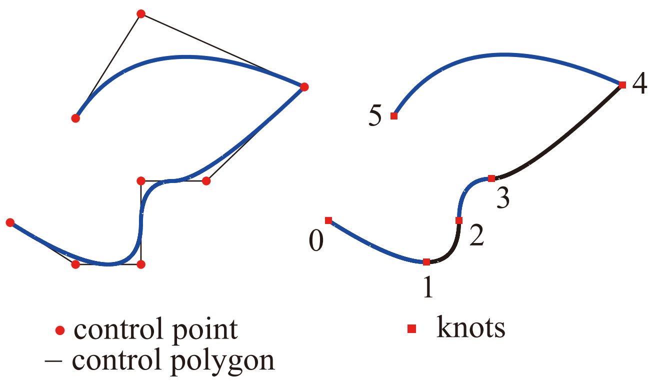

Figure 1. B-spline curve with control points, control polygon, and knots

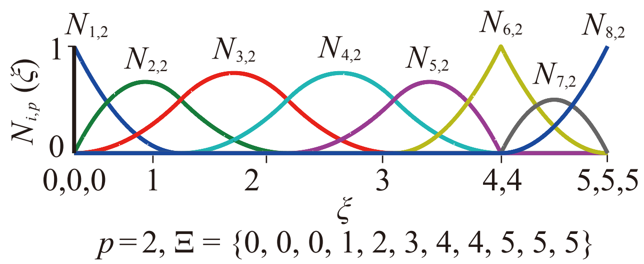

Figure 2. Quadratic B-spline basis function

An example B-spline curve is shown in Figure 1 with eight control points and $p = 2$; the resulting control polygon is shown in Figure1, and the B-spline basis functions are shown in Figure 2. Note that the curve is interpolatory at the first and last control points, due to the fact that the knot vector is open, and also at the sixth control point, due to the fact that the multiplicity of the knot $\xi = 4$ is equal to the polynomial order. Note also that the curve is tangent to the control polygon at the first, last and sixth control points. The curve is $C^{p\text{-}1}$-continuous everywhere except at the location of the repeated knot, $\xi = 4$, where it is $C^{p\text{-}2}$ (= C^0)-continuous.

To describe a two-dimensional B-spline, it is convenient to summarize the basis functions and their first-order derivative in a matrix form as follows:

$$\mathbf{N} = \begin{bmatrix} N_{1,p} & 0 & N_{2,p} & 0 & \cdots & N_{i,p} & 0 & \cdots & N_{n,p} & 0 \\ 0 & N_{1,p} & 0 & N_{2,p} & \cdots & 0 & N_{i,p} & \cdots & 0 & N_{n,p} \end{bmatrix} \tag{3}$$

$$\dot{\mathbf{N}} = \begin{bmatrix} \frac{dN_{1,p}}{d\xi} & 0 & \frac{dN_{2,p}}{d\xi} & 0 & \cdots & \frac{dN_{i,p}}{d\xi} & 0 & \cdots & \frac{dN_{n,p}}{d\xi} & 0 \\ 0 & \frac{dN_{1,p}}{d\xi} & 0 & \frac{dN_{2,p}}{d\xi} & \cdots & 0 & \frac{dN_{i,p}}{d\xi} & \cdots & 0 & \frac{dN_{n,p}}{d\xi} \end{bmatrix} \tag{4}$$

where the components in $\dot{\mathbf{N}}$ are given as

$$\frac{d}{d\xi}N_{i,p}(\xi)=\frac{p}{\xi_{i+p}-\xi_i}N_{i,p-1}(\xi)-\frac{p}{\xi_{i+p+1}-\xi_{i+1}}N_{i+1,p-1}(\xi) \tag{5}$$

Formulations in large deformation

The tangent stiffness matrix **K** is the sum of the linear stiffness matrix $\mathbf{K}_E$ and the geometrical stiffness matrix $\mathbf{K}_G$:

$$\mathbf{K}=\mathbf{K}_{\mathrm{E}}+\mathbf{K}_{\mathrm{G}} \tag{6}$$

The B-spline curves are used as shape functions for analysis of cable structures, thus, the formulations for $\mathbf{K}_E$ and the geometrical stiffness matrix $\mathbf{K}_G$ are given as [Bathe (1995)]

$$\mathbf{K}_{\mathrm{E}}=\frac{EAL_0}{2}\int_{\xi_1}^{\xi_n}\mathbf{B}^{\mathrm{T}}\mathbf{B}\,d\xi \tag{7}$$

$$\mathbf{K}_{\mathrm{G}}=\frac{AL_0}{2}\int_{\xi_1}^{\xi_n}\bar{\sigma}\,\mathbf{B}_{\mathrm{NL}}^{\mathrm{T}}\mathbf{B}_{\mathrm{NL}}\,d\xi \tag{8}$$

$$\mathbf{B}=\frac{4}{L^2}\mathbf{X}^{\mathbf{T}}\dot{\mathbf{N}}^{\mathbf{T}}\dot{\mathbf{N}} \tag{9}$$

$$\mathbf{B}_{\mathrm{NL}}=\frac{2}{L}\dot{\mathbf{N}} \tag{10}$$

$$\bar{\sigma}=E\bar{\varepsilon}=E\frac{4}{L^2}\mathbf{X}^{\mathbf{T}}\dot{\mathbf{N}}^{\mathbf{T}}\dot{\mathbf{N}}\mathbf{U} \tag{11}$$

$$\mathbf{U}=\mathbf{X}-\mathbf{X}^0 \tag{12}$$

$$\mathbf{X}^{\mathrm{T}}=\left[x_1,y_1,\cdots,x_i,y_i,\cdots,x_n,y_n\right] \tag{13}$$

$$\left(\mathbf{X}^0\right)^{\mathrm{T}}=\left[x_1^0,y_1^0,\cdots,x_i^0,y_i^0,\cdots,x_n^0,y_n^0\right] \tag{14}$$

Where E is Young's Modulus, A is the initial cross-sectional area, L_0 is the initial element length before deformation, L is the current length after deformation, $\bar{\sigma}$ is the axial stress in small deformation, $\bar{\varepsilon}$ is the axial strain in small deformation x_i, y_i are the current coordinates of the specified nodes of the element, and x_i^0, y_i^0 are the initial coordinates of the specified nodes of the element. For large deformation problems, the true axial strain has to be calculated from the extension of the cables, which is given as

$$\varepsilon=\frac{ds}{ds^0}-1=\sqrt{\left(\frac{dx}{ds^0}\right)^2+\left(\frac{dy}{ds^0}\right)^2}-1=\frac{2}{L_0}\sqrt{\left(\frac{dx}{d\xi}\right)^2+\left(\frac{dy}{d\xi}\right)^2}-1 \tag{15}$$

Structural analysis by singular value decomposition

Tangent stiffness matrix **K** of an unstable structure is not invertible, because it is singular. To proceed the analysis for unstable structures ruling out the mechanisms as well as rigid-body motions, which cause singularity of **K**, singular value composition of **K** turns out to be convenient for formulations as well as computations [Kawaguchi (2011)]. By using a unitary matrix **Ψ**, a (symmetric) tangent stiffness matrix **K** is rewritten as follows:

$$\mathbf{K} = \mathbf{\Psi} \begin{pmatrix} \lambda_1 & & & & & \\ & \ddots & & & \mathbf{O} & \\ & & \lambda_i & & & \\ & & & \lambda_{i+1} & & \\ & \mathbf{O} & & & \ddots & \\ & & & & & \lambda_{dof} \end{pmatrix} \mathbf{\Psi}^{\mathbf{T}} \tag{16}$$

where **O** is a zero matrix, λ_i is the i^{th} singular value of **K**, *dof* is the number of degrees of freedom of the system. The pseudo-inverse matrix $\mathbf{K}^-$ of the tangent stiffness matrix **K** is obtained as follows

$$\mathbf{K}^- = \mathbf{\Psi} \begin{pmatrix} 1/\lambda_1 & & & & & \\ & \ddots & & & \mathbf{O} & \\ & & 1/\lambda_i & & & \\ & & & 1/\lambda_{i+1} & & \\ & \mathbf{O} & & & \ddots & \\ & & & & & 1/\lambda_{dof} \end{pmatrix} \mathbf{\Psi}^{\mathbf{T}} \tag{17}$$

$$\text{if } \lambda_i = 0 \quad \text{then} \quad 1/\lambda_i = 0$$

Subjected to the external load **F**, the displacements of control points of a (unstable) cable structure can be calculated by using the $\mathbf{K}^-$ defined in Eq. (17) as follows:

$$\mathbf{U} = \mathbf{K}^- \mathbf{F} \tag{18}$$

Accuracy evaluation and initial settings for analysis

In this paper, we analyze the self-equilibrium shapes of the cable structures subjected to gravity, and verify the accuracy of the analyses, which is evaluated by the mean square error (MSE) defined as

$$\text{RSE} = \sqrt{\frac{1}{m}\sum_{i=1}^{m}\left(\frac{y_i - \overline{y}_i}{f}\right)^2} \times 100 \quad [\%] \tag{19}$$

where m is the number of evaluation points, y_i, $\overline{y}_i$ are respectively the i^{th} y-coordinate calculated by analysis and by theory, and f is sag of the cable.

In this paper, two cable structures with different initial shapes. Each of them are analyzed by different models:

- 9 two-node isoparametric elements with 10 nodes,
- 30 two-node isoparametric elements with 31 nodes,
- 9 four-node isoparametric elements with 10 (external) nodes,
- 30 four-node isoparametric elements with 31 (external) nodes,
- a single cubic B-spline curve with 10 control points, and
- a single cubic B-spline curve with 31 control points.

Two-node isoparametric elements are interpolated by straight lines, and four-node isoparametric elements are interpolated by cubic curves. To have the same (cubic) order for geometry description, the isogeometric elements are interpolated by the same polynomial order as four-node isoparametric elements. Young's Modulus E is 205[GPa], the initial cross-sectional area A is 0.0001[m^2], spatial span is 30[m], the weight of the cable per unit length μ for catenary cables is 7.85[N/m], the vertical distributed load w_0 for parabolic cables is 7.85[N/m], and the number of evaluation points of mean square error is 3000 points. CPU is 2.8 GHz Intel Core i7, the memory of the CPU is 12GB, and analysis software is MATLAB R2007b provided by MathWorks Corporation.

Self-equilibrium analysis of catenary cable

The self-equilibrium shape of a single cable against its own weight becomes a catenary [Japan Society of Civil Engineers (2001)]. In this section, a catenary is used as the exact solution. The formulation of symmetric catenary cable is give as

$$y = \frac{T_0}{\mu}\cosh\left(\frac{\mu x}{T_0}\right) \tag{20}$$

where x, y is x-coordinate and y-coordinate respectively, T_0 is the horizontal tension.

(a) two-node elements **(b) four-node elements** **(c) cubic B-spline elements**

Figure 3. Initial catenary cable of object 1 with 10 nodes

(a) two-node elements **(b) four-node elements** **(c) cubic B-spline elements**

Figure 4. Final catenary cable of object 1 with 10 nodes

(a) two-node elements **(b) four-node elements** **(c) cubic B-spline elements**

Figure 5. Initial catenary cable of object 2 with 10 nodes

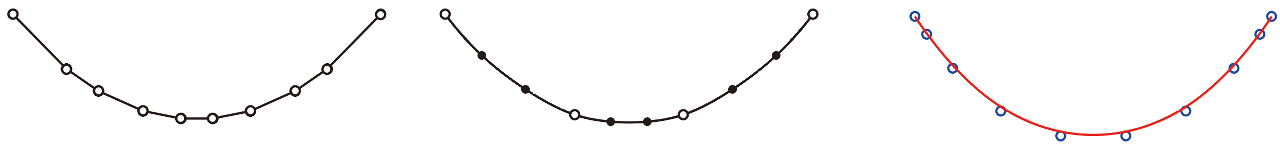

(a) two-node elements **(b) four-node elements** **(c) cubic B-spline elements**

Figure 6. Final catenary cable of object 2 with 10 nodes

(a) two-node elements **(b) four-node elements** **(c) cubic B-spline elements**

Figure 7. Initial catenary cable of object 1 with 31 nodes

(a) two-node elements **(b) four-node elements** **(c) cubic B-spline elements**

Figure 8. Final catenary cable of object 1 with 31 nodes

(a) two-node elements **(b) four-node elements** **(c) cubic B-spline elements**

Figure 9. Initial catenary cable of object 2 with 31 nodes

(a) two-node elements **(b) four-node elements** **(c) cubic B-spline elements**

Figure 10. Final catenary cable of object 2 with 31 nodes

Table 1. Identified results of catenary cable

The number of nodes	Object	Element	The number of iterations	MSE[%]	Analysis time [s]
10 nodes	1	two-node	14 times	1.0620	0.2274
		four-node	27 times	0.0206	0.1843
		B-spline	26 times	0.0070	0.1247
	2	two-node	20 times	0.9425	0.3150
		four-node	93 times	0.5024	0.6957
		B-spline	37 times	0.2553	0.1767
31 nodes	1	two-node	21 times	0.0992	0.8055
		four-node	27 times	0.0023	1.1661
		B-spline	46 times	0.0019	2.0281
	2	two-node	79 times	0.0897	2.5160
		four-node	45 times	0.0165	1.9095
		B-spline	76 times	0.0052	3.2307

The initial shapes from which the large deformation analysis for different modeling are shown in Figures 3, 5, 7, and 9, and their corresponding final shapes due to gravity are respectively shown in Figures 4, 6, 8, and 10. Note that in (a) and (b) in these figures, ○ refers to element boundary node, ● refers to element internal node; and moreover, in (c) in these figures, ○ refers to control point.

Performances of the analyses using conventional FEA as well as IGA with different number of elements are summarized in Table 1. It was clear that IGA is more accurate compared to conventional FEA when the structure is modeled by using the same (external) nodes (or control points for IGA). On the other hand, convergence performance of IGA is not superior to that of conventional FEA.

Self-equilibrium analysis of parabolic cable

The self-equilibrium shape of cable with large vertical distributed load compared to its own weight becomes a parabolic cable. Parabolic cables are widely used in design of suspension bridges. In the analysis, the weight of the cable is regarded as zero and vertical distributed loads like floor slabs of the bridge are treated as loads applied to the nodes. The formulation of a symmetric parabolic cable is given as

$$y = \frac{w_0}{2T_0} x^2 \tag{21}$$

The initial shapes from which the large deformation analysis for different modeling are shown in Figures 11, 13, 15, and 17, and their corresponding final shapes due to gravity are respectively shown in Figures 12, 14, 16, and 18. Note that in (a) and (b) in these figures, ○ refers to element boundary node, ● refers to element internal node; and moreover, in (c) in these figures, ○ refers to control point.

(a) two-node elements **(b) four-node elements** **(c) cubic B-spline elements**

Figure 11. Initial parabolic cable of object 1 with 10 nodes

(a) two-node elements **(b) four-node elements** **(c) cubic B-spline elements**

Figure 12. Final parabolic cable of object 1 with 10 nodes

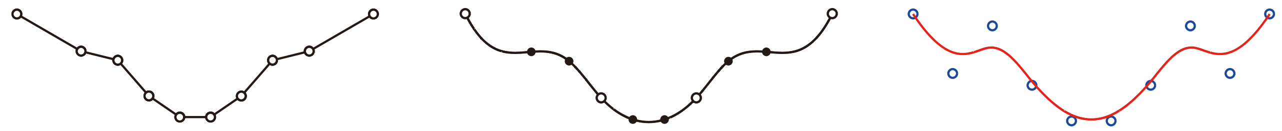

(a) two-node elements **(b) four-node elements** **(c) cubic B-spline elements**

Figure 13. Initial parabolic cable of object 2 with 10 nodes

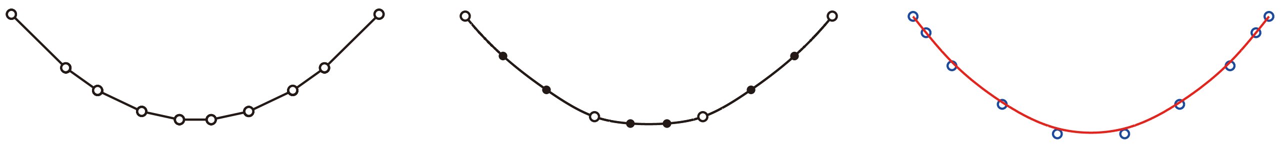

(a) two-node elements **(b) four-node elements** **(c) cubic B-spline elements**

Figure 14. Final parabolic cable of object 2 with 10 nodes

(a) two-node elements **(b) four-node elements** **(c) cubic B-spline elements**

Figure 15. Initial parabolic cable of object 1 with 31 nodes

(a) two-node elements **(b) four-node elements** **(c) cubic B-spline elements**

Figure 16. Final parabolic cable of object 1 with 31 nodes

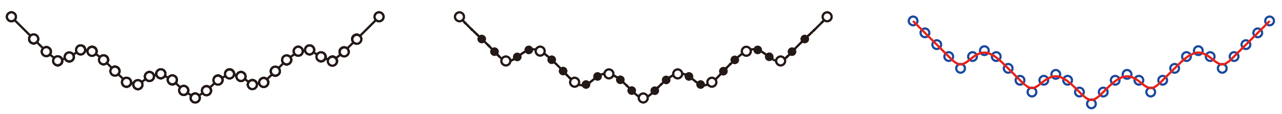

(a) two-node elements **(b) four-node elements** **(c) cubic B-spline elements**

Figure 17. Initial parabolic cable of object 2 with 31 nodes

(a) two-node elements **(b) four-node elements** **(c) cubic B-spline elements**

Figure 18. Final parabolic cable of object 2 with 31 nodes

Table 2. Identified results of parabolic cable

The number of nodes	Object	Element	The number of iterations	MSE[%]	Analysis time [s]
10 nodes	1	two-node	14 times	1.0521	0.2424
		four-node	26 times	0.6397	0.1984
		B-spline	25 times	0.3134	0.3075
	2	two-node	23 times	0.8808	0.3816
		four-node	85 times	0.6589	0.6553
		B-spline	42 times	0.1681	0.2186
31 nodes	1	two-node	21 times	0.0979	0.9618
		four-node	31 times	0.0856	0.7811
		B-spline	36 times	0.0838	1.4093
	2	two-node	325 times	0.0949	14.3975
		four-node	53 times	0.0873	1.2747
		B-spline	84 times	0.0860	3.2134

Performances of the analyses using conventional FEA as well as IGA with different number of elements are summarized in Table 2. It was clear that IGA performs better than conventional FEA in accuracy in all cases. However, the superiority of IGA in computation costs is not clear.

Conclusions

In this paper, we applied Isogeometric Analysis for self-equilibrium analysis of unstable cable structures and investigated its performances in accuracy as well as in efficiency. For all analysis cases in this paper both for catenary cables and parabolic cables, IGA is more accurate than conventional FEA. However, its performance on computational costs is not as clear as accuracy.

References

T.J.R. Hughes, J.A. Cottrell, Y. Bazilevs (2005) Isogeometric analysis: CAD, finite elements, NURBS, exact geometry and mesh refinement

J. Austin Cottrell, Thomas J. R. Hughes, Yuri Bazilevs (2009) Isogeometric Analysis: Toward Integration of CAD and FEA

Stefan Hartmann, David J. Benson, David Lorenz (2011) About Isogeometric Analysis and the new NURBS-based finite Elements in LS-DYNA, *8th European LS-DYNA Users Conference*

D.J. Benson, Y. Bazilevs, M.C. Hsu, T.J.R. Hughes (2010) Isogeometric shell analysis: Yhe Reissner-Mindlin shell, *Compt. Methods Appl. Mech. Engrg.* **199**, 276-289

Klaus-Jurgen Bathe (1995) Finite Element Procedures

Japan Society of Civil Engineers (2001) Fundamentals and Applications of cable space structures

Ken'ichi Kawaguchi (2011) generalized inverse matrix and application to structural engineering (Computational Engineering Series)